A physics-based TCAD framework for the noise analysis of RF CMOS circuits under the large signal operation

Sung-min Hong, Raseong Kim, Chan Hyeong Park*, Hong Shick Min, and Young June Park

School of EECS and Nano-Systems Institute (NSI-NCRC), Seoul National University, Seoul, Korea
*School of Electronics Engineering, Kwangwoon University, Seoul, Korea
Telephone: +82-2-880-7285, Fax: +82-2-882-4658, E-mail: hi2ska2@isis.snu.ac.kr

Abstract

We have developed a general TCAD framework for the large-signal noise analysis of the RF (radio-frequency) CMOS circuits and applied it to the single-balanced mixer, as an example. Using the conversion Green's function method, the effect of the modulated noise sources in the devices on the cyclostationary mixer output noise voltage is simulated. It is shown that the newly-developed general TCAD framework for the mixed device-circuit environment can give a physics-based and efficient large-signal (LS) noise simulation.

Keywords: cyclostationary noise, RF CMOS mixer, conversion Green's function, TCAD framework and large-signal condition

Introduction

The mixer, which "mixes" a large local oscillator (LO) signal and a small RF signal, is an indispensable circuit for frequency-translation in RF applications such as the transceiver front-end. In such cases, the noise characteristic of the mixer is critical to the system performance and an accurate noise analysis of the mixer is needed. Since the mixer is under the large periodic signal operation, the stationary noise analysis technique which considers only the dc steady-state cannot be applied for the mixer noise analysis and a viewpoint of the linear periodically time varying (LPTV) system should be considered, where the system inputs are diffusion noise sources and system output is mixer noise voltage. Although mixer noise analyses have been made through a transient simulation by SPICE [1] or by an analytical approach [2], a rigorous physics-based mixer noise simulation has not been reported yet. In this work, we report a physics-based analysis of noise in the RF CMOS single-balanced mixer for the first time.

Simulation Framework

We have developed a general TCAD framework [3] for the simulation of the RF device-circuit environment. In this framework, the devices are discretized as in the conventional device simulators. The semiconductor equations (i.e. Poisson equation and the electron and hole continuity equations) are solved in the frequency domain using the harmonics balance (HB) technique [4]. The iterative matrix solver, generalized minimum residual method (GMRES), is exploited since the size of the system is too large to deal with the direct solver. We use the 'quasi-static Jacobian,' which neglects the time derivatives of the governing equations for the system including the semiconductor equations, as a prescaler. We find out that the method is very effective and numerically efficient in decoupling the components originated from different sampled components in the time domain up to a few hundreds GHz range.

For the noise analysis, the system is linearized to get the conversion Green's functions (CGFs) by an aid of the generalized adjoint approach [5]. Although there have been papers which showed the LS noise simulation [5,6], to authors' knowledge, our approach is the first one successfully applied to the moderately large system such as the real RF mixer with the two-dimensional MOSFETs and our framework can be applied to the even larger systems without convergence problem. This can be possible by the effective utilization of the prescaler as described above.

Simulation Results and Discussion

The circuit schematic considered in the simulation is shown in Fig. 1. Simulation has been carried out on the single-balanced RF CMOS mixer whose output signal is taken as a differential voltage. The mixer consists of two resistors and three nMOSFETs and the number of the unknowns per a sampling time is about 24,000. Since the number of the harmonics is set to 10, the whole system has about a half million unknowns. The magnitude and fundamental frequency of the LO signal is 0.15 V and 1 GHz, respectively. In Fig. 2, we can see the magnitudes of the Fourier coefficients of the mixer output voltage. The LO signal and the output voltages are plotted in the time domain in Fig. 3. Also in Fig. 4, the electron concentration at the oxide-silicon interface in the left LO port MOSFET is shown for a period of 1 nsec.

Based upon the simulated LS solution, the response of the LPTV system to the RF input signal is evaluated. We select 0.1 GHz as the sideband frequency. Fig. 5 depicts the response of the mixer output voltage at 0.1 GHz frequency to the RF input signal at various frequencies. From this figure, we can find that the conversion gain for the 1.1 GHz RF signal is 1.33.

The CGF for the mixer output noise voltage at 0.1 GHz frequency corresponding to the (modulated) electron noise source is calculated. Fig. 6 shows the CGF for 1.1 GHz noise source in the RF port MOSFET. The noise source in the drain side has strong impact on the mixer output noise. Fig. 7 also shows the same quantity in the left LO port MOSFET. Contrary to Fig. 6, the noise source in the source side has a strong impact on the mixer output noise since the frequency down-conversion from 1.1 GHz to 0.1 GHz takes place in the channel in the LO port MOSFET. In addition, the CGFs for 0.1 GHz noise source (no frequency conversion) in the RF port and LO port MOSFET are shown in Figs. 8 and 9, respectively. The effect of the noise source only in the drain side of the LO port MOSFET is found to be dominant because the frequency conversion is not needed in this case. In Fig. 10 we plot the CGFs along the channel in the RF port MOSFET at various frequencies. Fig. 11 shows the same quantities in the LO port MOSFET. The sideband correlation matrix (SCM) elements of the diffusion noise source for electron continuity equation at the center of the channel in the LO port MOSFET are plotted in Fig. 12. Here the 'Frequency index,' n, means (n–5.9) GHz. We note that the off-diagonal components have significant magnitudes, which means that the cross-correlation between the two distinct frequencies cannot be neglected.

Fig. 13 shows the spatial contribution to the mixer output noise voltage in the RF port MOSFET. Also the spatial contribution in the LO port MOSFET is shown in Fig. 14. The power spectral density of the mixer output noise voltage is calculated to be 20.2 $(nV)^2$/Hz, among which 55 % comes from the RF port MOSFET and the other comes from the LO port MOSFETs (the noise from two resistors are not considered).

Finally, we calculate the mixer output noise voltage at various LO signal amplitudes (0.1, 0.15, 0.2, 0.25 V). Fig. 15 shows the simulated mixer output voltages in the time domain. Also the conversion gains and power spectral densities of the mixer output noise voltage are shown in Fig. 16.

Conclusion

In this work, we have developed a general TCAD framework for the LS noise analysis of the CMOS RF circuits. The noise characteristic of the RF CMOS single-balanced mixer has been simulated. We expect that this framework can be extended for the physics-based and efficient LS noise analysis of general RF CMOS circuits.

References

[1] C. D. Hull and R. G. Meyer, *IEEE Trans. Circuits and Systems – I : Fundamental Theory and Applications*, vol. 40, pp. 909-919, 1993.

[2] F. Danneville, G. Dambrine and A. Cappy, *IEEE Trans. Electron Devices*, vol. 45, pp. 2207-2212, 1998.

[3] S.-m. Hong, "CLESICO (Circuit Level Simulation Code) manual," unpublished.

[4] B. Troyanovsky, Ph.D. Dissertation, Stanford University, 1997.

[5] F. Bonani, S. D. Guerrieri, G. Ghione and M. Pirola, *IEEE Trans. Electron Devices*, vol. 48, pp. 966-977, 2001.

[6] J. E. Sanchez, Gijs Bosman and M. E. Law, *IEEE Trans. Electron Devices*, vol. 50, pp. 1353-1362, 2003.

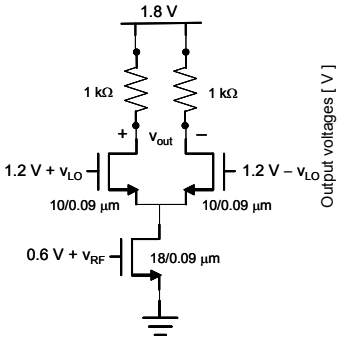

Fig. 1 Schematic of the mixer circuit simulated.

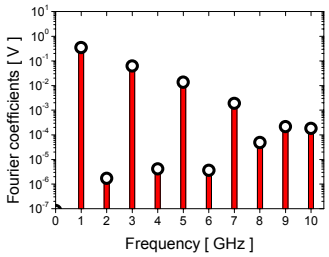

Fig. 2 Magnitudes of Fourier coefficients of the mixer output voltage.

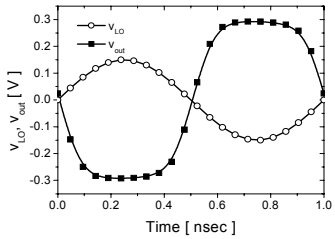

Fig. 3 LO signal and the mixer output voltage in the time domain.

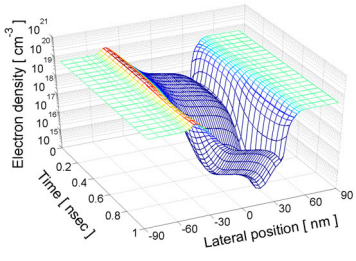

Fig. 4 Electron concentration at oxide-silicon interface in the left LO port MOSFET as a function of time.

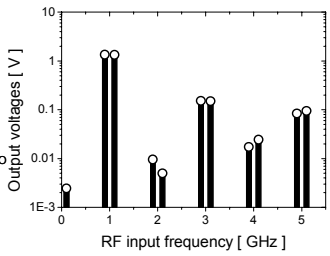

Fig. 5 Response of output voltage at 0.1 GHz to the RF input signal.

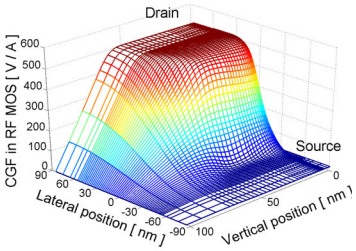

Fig. 6 CGF for 1.1 GHz noise source in the RF port MOSFET.

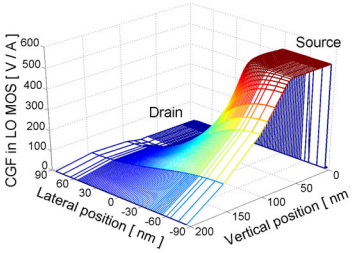

Fig. 7 CGF for 1.1 GHz noise source in the left LO port MOSFET.

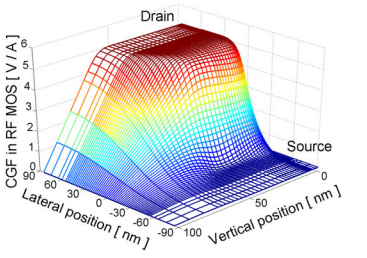

Fig. 8 CGF for 0.1 GHz noise source in the RF port MOSFET. Note that the magnitude is much smaller than that of Fig. 6.

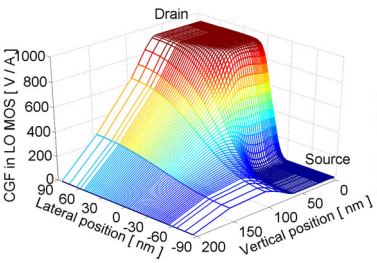

Fig. 9 CGF for 0.1 GHz noise source in the left LO port MOSFET.

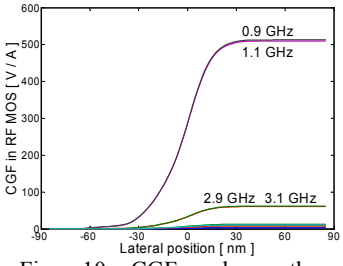

Fig. 10 CGFs along the channel in the RF port MOSFET at various frequencies.

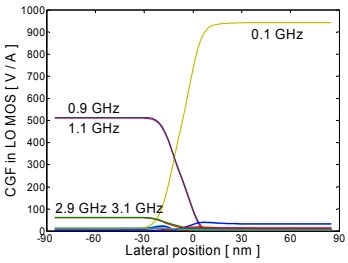

Fig. 11 CGFs along the channel in the LO port MOSFET at various frequencies.

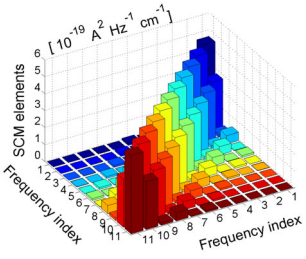

Fig. 12 SCM elements of the diffusion noise source at the center of the channel in the LO port MOSFET. Here the 'Frequency index,' n, means (n–5.9) GHz.

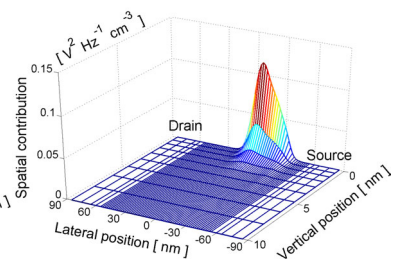

Fig. 13 Spatial noise contribution of the RF port MOSFET.

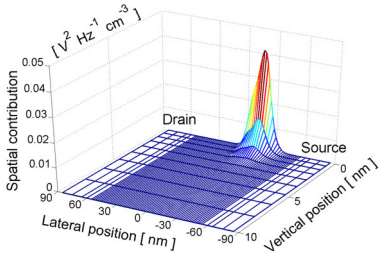

Fig. 14 Spatial noise contribution of the LO port MOSFET.

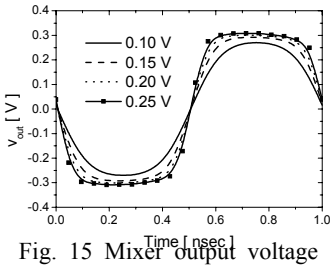

Fig. 15 Mixer output voltage in the time domain at various LO signal amplitudes (0.1, 0.15, 0.2, 0.25 V).

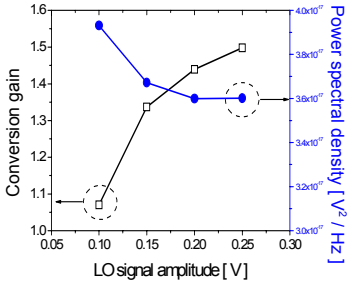

Fig. 16 Conversion gains and power spectral densities as functions of the LO signal amplitudes.